Electronic Supplementary Material (ESI) for Journal of Materials Chemistry A.

Controllably Electrolytic Formation of Ti_2O as Efficient Sulfur Host in lithium-sulfur (Li-S) battery

Ruxing Wang[a], Kangli Wang[a], Hongwei Tao[a], Wenjie Zhao[b], Mao Jiang[b], Jie Yan [b], Kai Jiang[a*]*

[a]*State Key Laboratory of Advanced Electromagnetic Engineering and Technology, School of Electrical and Electronic Engineering, Huazhong University of Science and Technology, Wuhan, Hubei 430074, China.*

[b]*State Key Laboratory of Materials Processing and Die & Mould Technology, School of Materials Science and Engineering, Huazhong University of Science and Technology, Wuhan, Hubei 430074, China.*

E-mail: kjiang@hust.edu.cn; klwang@hust.edu.cn

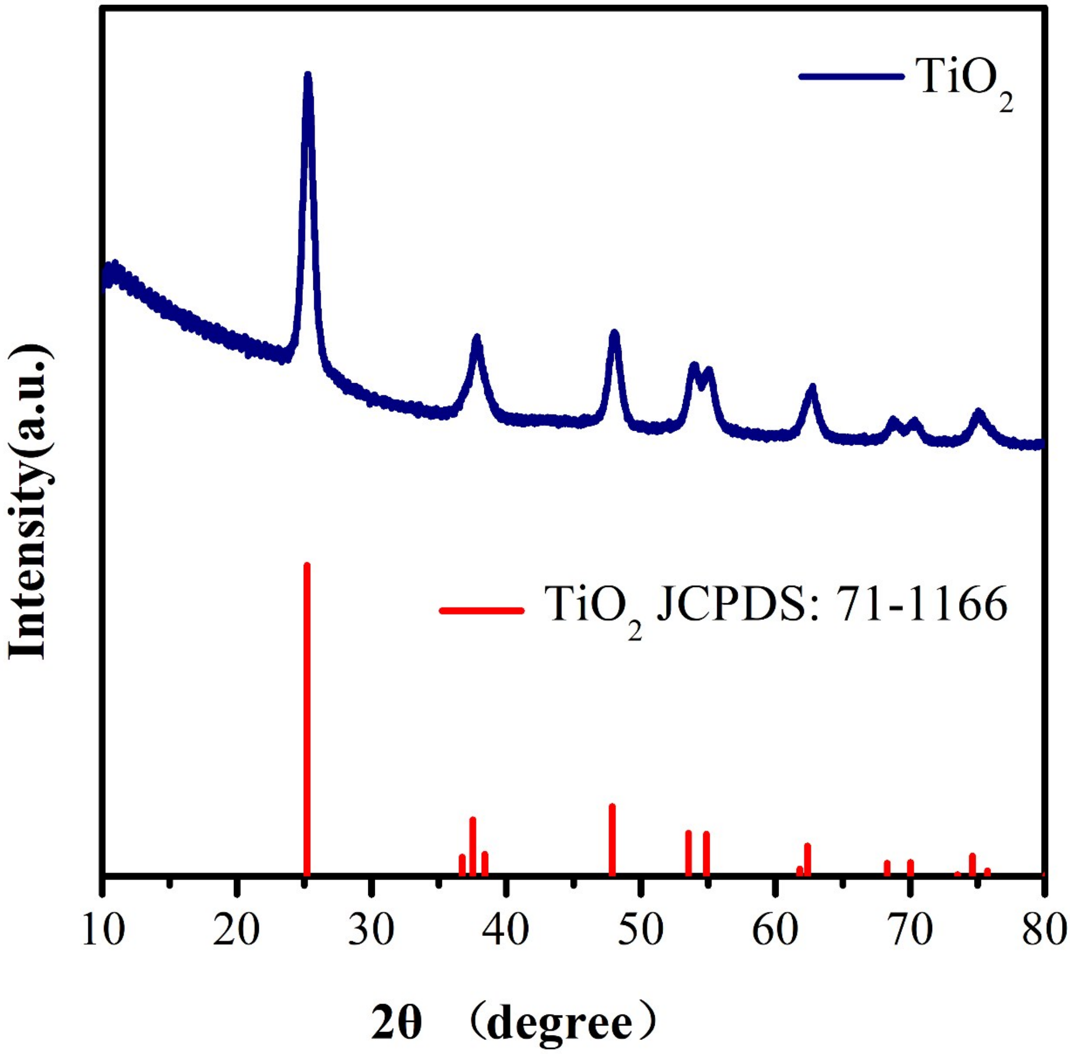

Figure S1. XRD patterns of the pristine TiO_2

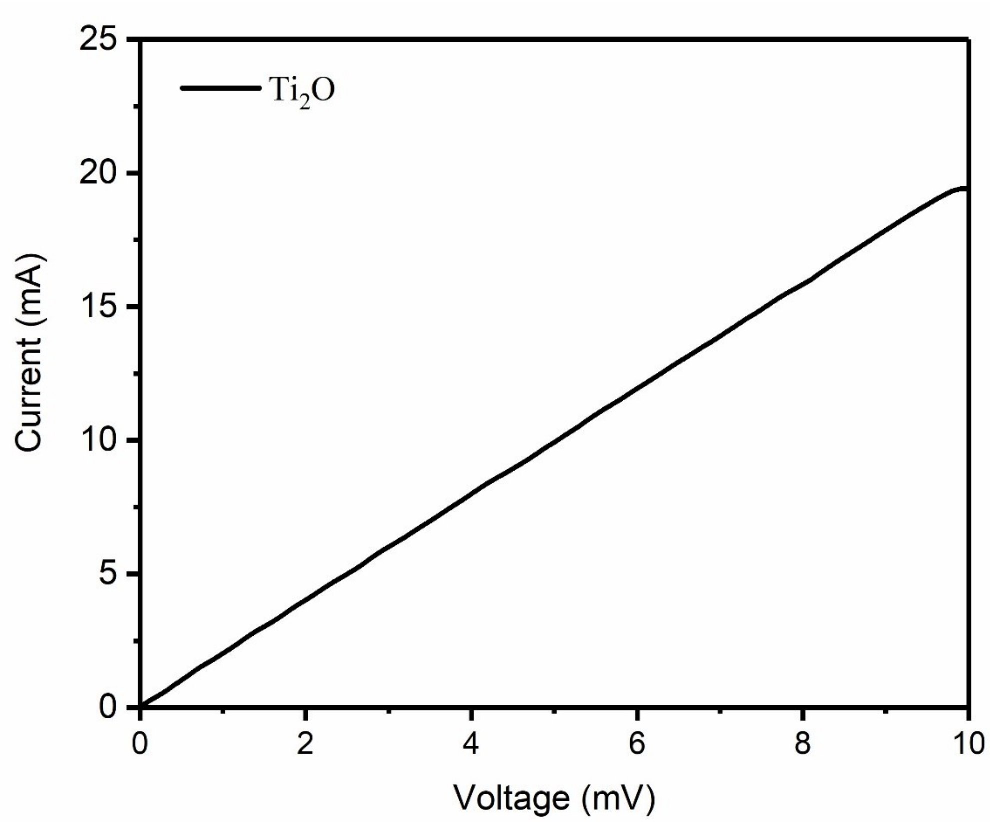

Figure S2. Electronic conductivity of the as-prepared Ti_2O. Based on the I-V analysis, the electronic conductivity of Ti_2O is calculated to be 296.8 S m^{-1}.

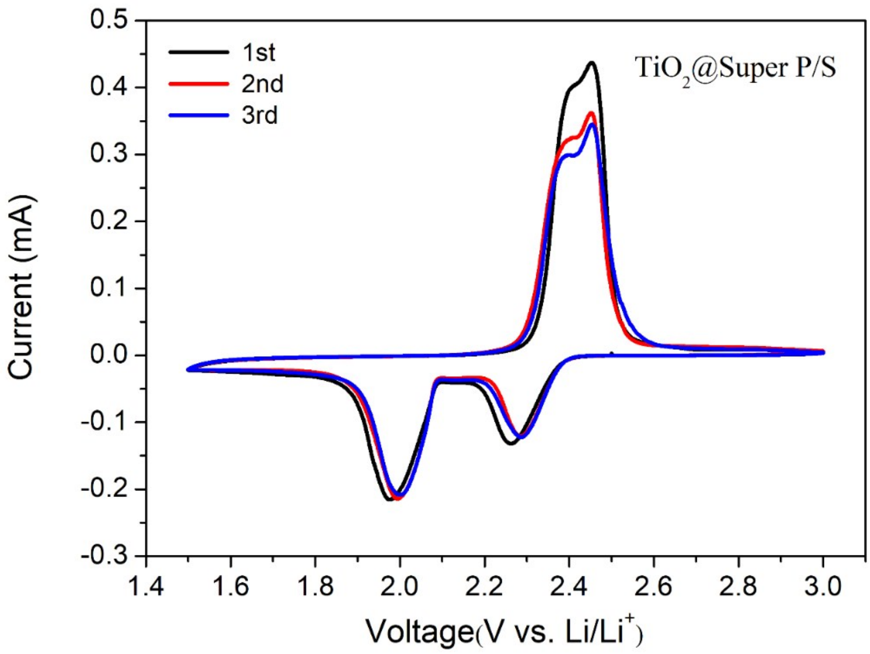

Figure S3. CV curves of the initial four cycles of the TiO_2@super P/S cathode at a scan rate of 0.1 mV s^{-1}.

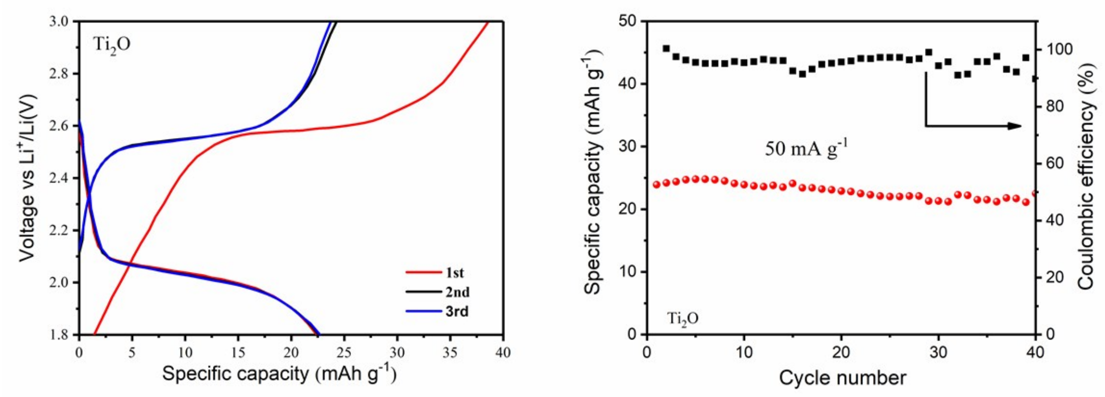

Figure S4 Charge/discharge curves of the Ti_2O cathode and the corresponding cycle performance at 50 mA g^{-1}.

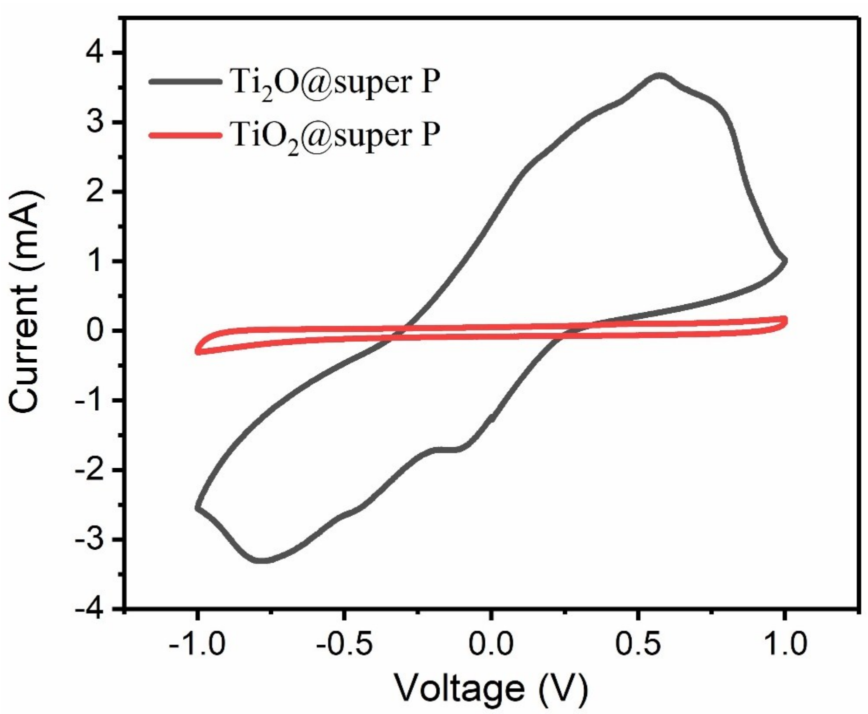

Figure S5. CV of symmetric cells. Fig. S7 Cyclic voltammograms of Li_2S_4 symmetric cells.

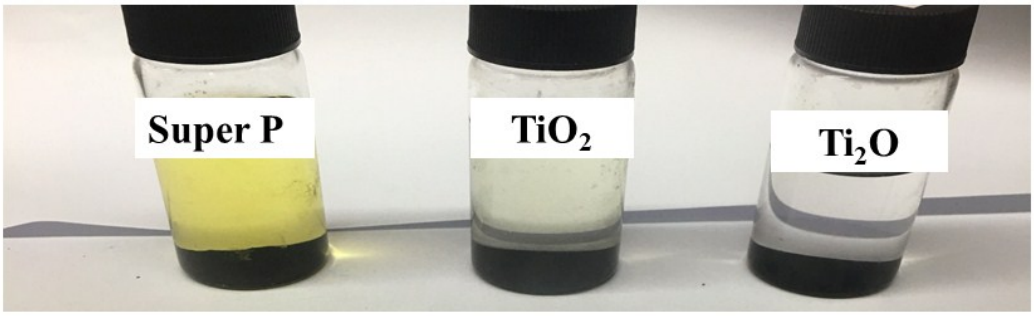

Figure S6. Li_2S_6 solution with Super P, TiO_2 or Ti_2O after resting for 1 h.

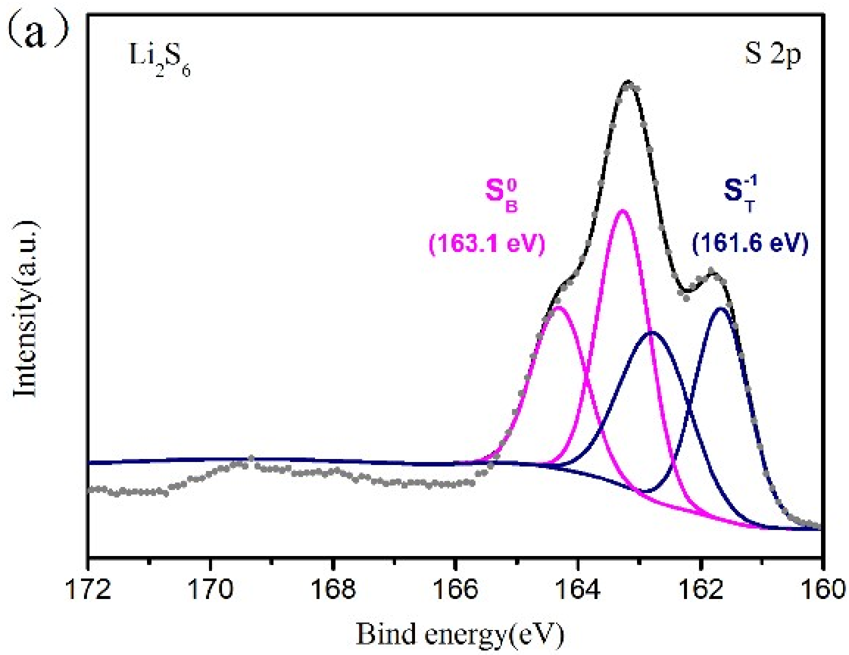

Figure S7. S 2p XPS spectra of Li_2S_6.

Theoretical calculation: The adsorptions of Li_2S_4 on Ti_2O and TiO_2 surfaces were investigated by the Vienna Ab-initio Simulation Package (VASP). The exchange-correlation function was described by the Perdew-Burke-Ernzerhof (PBE) of the generalized gradient approximation (GGA). The PAW pseudo-potential was used to describe the interaction between valence electrons and the ionic core. 3 × 3 {001} supercell with two Ti-O layers and 2 × 3 {101} supercell with eight Ti-O layers were used to simulate the surfaces of Ti_2O and TiO_2. The plane-wave basis with energy cutoff of 400 eV and the energy convergence of 1.0×10^{-5} eV were applied to the calculations of geometry optimization. Considering the computational cost, the geometry optimization calculations were only performed at the gamma point.

In the test, 0.05 M Li_2S_6 solution was placed in the left side of the cell, equal amount blank solvent was put in the right side. A G/Ti_2O or PP separator was placed at the bridge of the device.

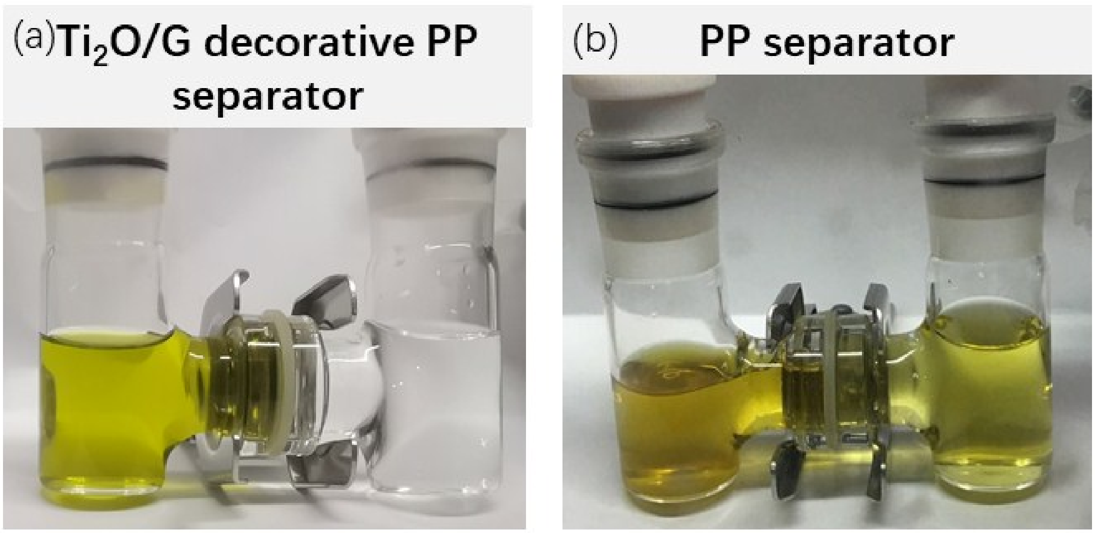

Figure S8. The verification of polysulfide immobilization with G/Ti_2O decorated separator (a) and commercialized PP separator (b) after resting for 5 hours.

The illustration of the fitting unit of the equivalent circuits for EIS fitting:

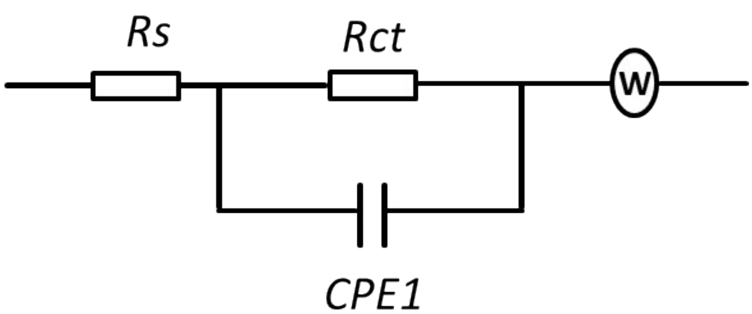

Figure S9. The equivalent circuits for EIS fitting before cycling test.

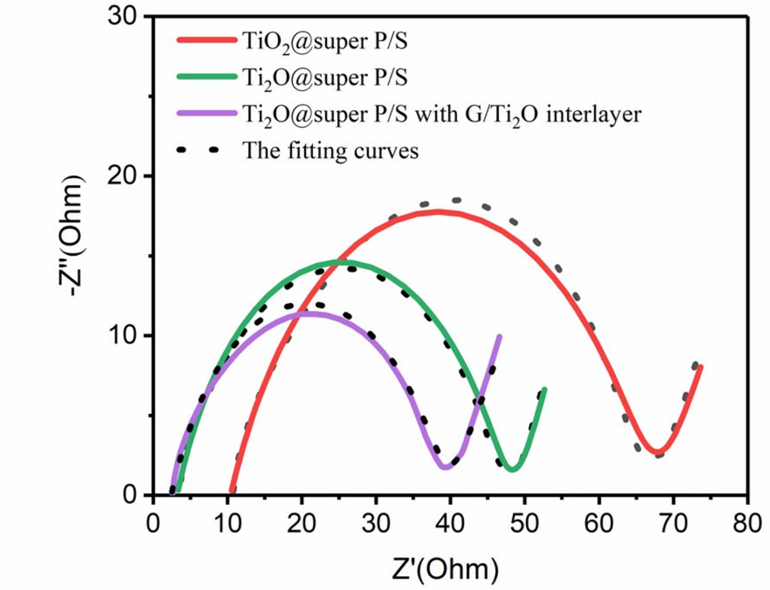

Figure S10 The Nyquist plots of the TiO_2@super P/S, Ti_2O@super P/S electrode and Ti_2O@super P/S with G/Ti_2O decorated separator cathode. The lines represent the measured results, and the dots correspond to the fitting curves.

Table S1 The fitting results of the electrochemical impedance spectroscopy

	Rs (Ω)	Rct (Ω)
TiO_2@super P/S	10.4	54.4
Ti_2O@super P/S	3.2	43.5
Ti_2O@super P/S with G/Ti_2O decorated separator	2.4	35.4

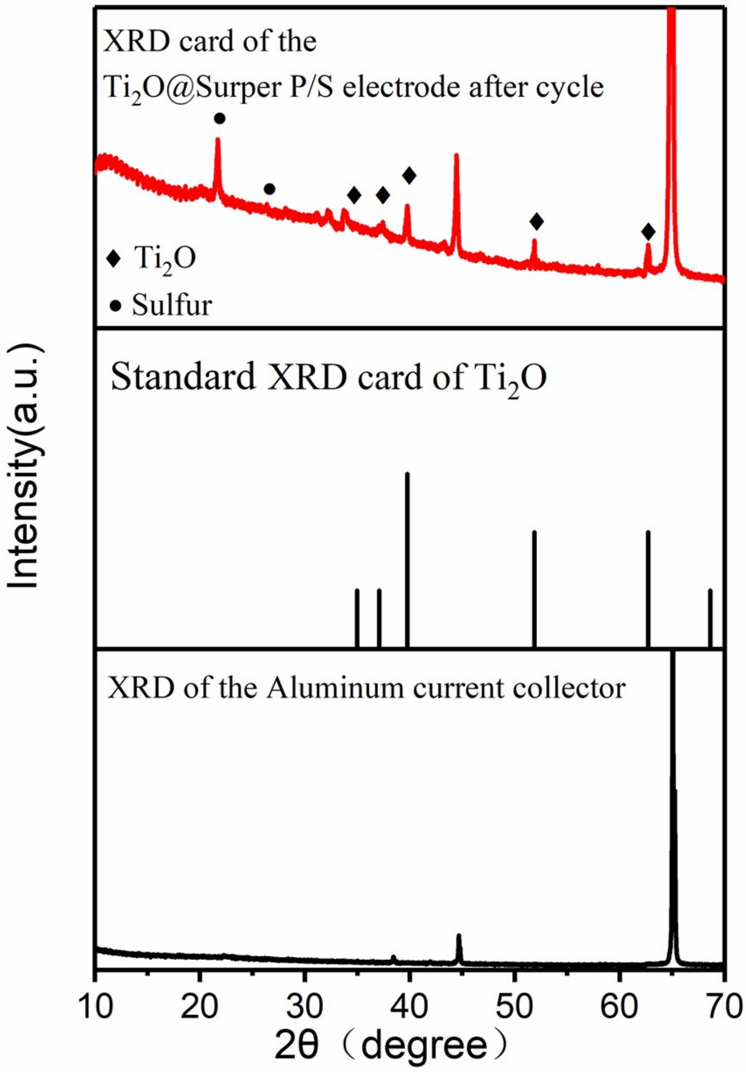

Figure S11 Ex situ XRD patterns of TiO_2@super P/S electrode after 500 cycles.

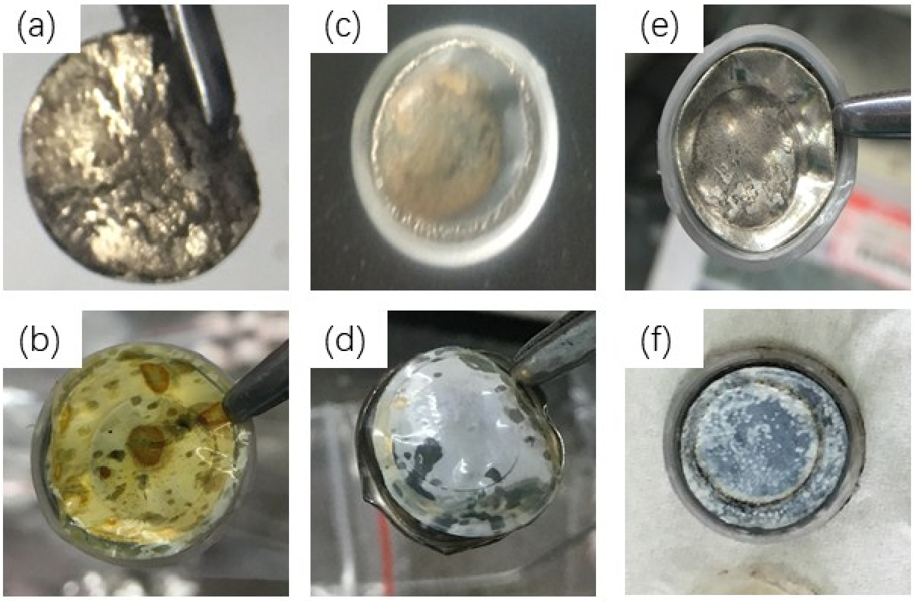

Figure S12. Lithium sheets and separators toward the side of the lithium sheet after cycled. (a) (b) TiO_2@super P/S cell, (c) (d) Ti_2O@super P/S cell, (e) (f)Ti_2O@super P/S with G/Ti_2O decorated separator

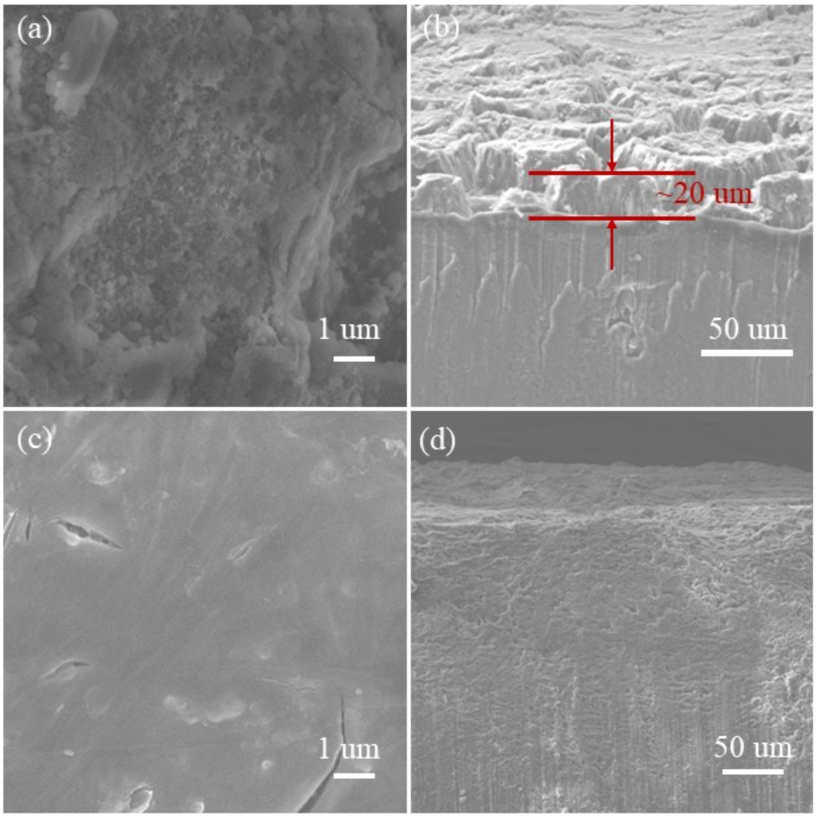

Figure S13 SEM images of battery components after tests. The surface morphologies of the Li anode that facing the TiO_2@super P/S (a) and Ti_2O@super P/S with G/Ti_2O decorated separator (c) cathodes, and the corresponding cross-sections (b) (d).

Table S2. Electrochemical properties comparison of our work with other Ti-Based Oxides for Lithium-Sulfur Batteries

Cathode hosts	Areal active material mass loading	Current Rate	Initial capacity [mAh g^{-1}]	cycles	Retention/ fading rate [%]	Reference
CNT@TiO_{2-x}-S [1]	~2.2	0.2	1204	150	72.01/0.19	*Adv. Energy Mater.* 2019
TiO_2-Ar/S [2]	NA	0.2	1472	100	61.14/0.39	*J. Mater. Chem. A*, 2019
S@3S-TiO_{2-x} [3]	~0.5	0.5	903	1000	79	*Angew. Chem.* 2019
TiO@C-HS [4]	~1.5	0.5	1066	500	0.08	*Nat. Commun*, 2016
HCS@Ti_4O_7/S [5]	NA	0.5	1168	800	76/0.06	*J. Mater. Chem. A*, 2019
H-TiO_x@S/ppy [6]	~1.0	1.0C	693.7	1000	59.35/0.04	ACS Appl. Mater. Interfaces 2019
$TinO_{2n-1}$@C/S [7]	~2.3	1.0C	700	1000	0.06	ChemSusChem 2018
C@TiO2@C-S [8]	~2.5	0.5C	999	300	74/0.086	*J. Mater. Chem. A*, 2018
Ti_2O_3-MA/S [9]	~1.5	0.5C	1060	250	81.1/0.08	ACS Appl. Mater. Interfaces 2019
Ti_2O@Super P /S	~2.5	0.5C	1063	500	81.1/0.04	This work

Reference

[1] Y. Wang, R. Zhang, J. Chen, H. Wu, S. Lu, K. Wang, H. Li, C. J. Harris, K. Xi and R. V. Kumar, *Advanced Energy Materials*, 2019, **9**, 1900953.

[2] H.-E. Wang, K. Yin, N. Qin, X. Zhao, F.-J. Xia, Z.-Y. Hu, G. Guo, G. Cao and W. Zhang, *Journal of Materials Chemistry A*, 2019, **7**, 10346-10353.

[3] E. H. M. Salhabi, J. Zhao, J. Wang, M. Yang, B. Wang and D. Wang, *Angewandte Chemie*, 2019.

[4] Z. Li, J. Zhang, B. Guan, D. Wang, L.-M. Liu and X. W. D. Lou, *Nature communications*, 2016, **7**, 13065.

[5] F. Wang, X. Ding, R. Shi, M. Li, Y. Lei, Z. Lei, G. Jiang, F. Xu, H. Wang and L. Jia, *Journal of Materials Chemistry A*, 2019, **7**, 10494-10504.

[6] G. Chen, W. Zhong, Y. Li, Q. Deng, X. Ou, Q. Pan, X. Wang, X. Xiong, C. Yang and M. Liu, *ACS applied materials & interfaces*, 2019, **11**, 5055-5063.

[7] U. Zubair, J. Amici, C. Francia, D. McNulty, S. Bodoardo and C. O'Dwyer, **ChemSusChem**, 2018

[8] M. Fang, Z. Chen, Y. Liu, J. Quan, C. Yang, L. Zhu, Q. Xu and Q. Xu, *J. Mater. Chem. A*, 2018, **6**, 1630-1638.

[9] P. Zeng, M. Chen, S. Jiang, Y. Li, X. Xie, H. Liu, X. Hu, C. Wu, H. Shu and X. Wang, *ACS applied materials & interfaces*, 2019.